Surface Microphase Separation in PDMS-*b*-PMMA-*b*-PHFBMA Triblock Copolymer Films

Ke-Jian Lian,[1] Chang-Qing Chen,[1] Hui Liu,[1] Ning-Xing Wang,[2] Hai-Jiang Yu,[2] Zheng-Hong Luo[2]

[1]*Department of Orthopedic, the Affiliated Southeast Hospital of Xiamen University, Orthopaedic Trauma Center of PLA, Zhangzhou 363000, People's Republic of China*
[2]*Department of Chemical and Biochemical Engineering, College of Chemistry and Chemical Engineering, Xiamen University, Xiamen 361005, People's Republic of China*

Received 28 July 2009; accepted 25 April 2010
DOI 10.1002/app.32682
Published online 13 October 2010 in Wiley Online Library (wileyonlinelibrary.com).

ABSTRACT: Well-defined poly(dimethylsiloxane)-*block*-poly(methyl methacrylate)-*block*-poly(2,2,3,3,4,4,4-heptafluorobutyl methacrylate) (PDMS-*b*-PMMA-*b*-PHFBMA) triblock copolymers were synthesized via atom transfer radical polymerization (ATRP). Surface microphase separation in the PDMS-*b*-PMMA-*b*-PHFBMA triblock copolymer films was investigated. The microstructure of the block copolymers was investigated by transmission electron microscopy (TEM) and atomic force microscopy (AFM). Surface composition was studied by X-ray photoelectron spectroscopy (XPS). The chemical composition at the surface was determined by the surface microphase separation in the PDMS-*b*-PMMA-*b*-PHFBMA triblock copolymer films. The increase of the PHFBMA content could strengthen the microphase separation behavior in the PDMS-*b*-PMMA-*b*-PHFBMA triblock copolymer films and reduce their surface tension. Comparison between the PDMS-*b*-PMMA-*b*-PHFBMA triblock copolymers and the PDMS-*b*-PHFBMA diblock copolymers showed that the introduction of the PMMA segments promote the fluorine segregation onto the surface and decrease the fluorine content in the copolymers with low surface energy. © 2010 Wiley Periodicals, Inc. J Appl Polym Sci 120: 156–164, 2011

Key words: microphase separation structure; PDMS-*b*-PMMA-*b*-PHFBMA triblock copolymer; AFM

INTRODUCTION

Block or segmented copolymers have different blocks. The dissimilar nature of these blocks combined with the fact that they are chemically linked to each other manifests in a variety of surface and bulk properties quite different from those of the corresponding homopolymeric system.[1,2] The surface properties of block copolymers originate from the difference in the surface free energies of the components blocks. As a whole, in a block copolymer system, segments of lower surface free energy tend to enrich the surface of a condensed phase. Thus in a phase-separated block copolymer, segments with lower surface free energy preferentially segregate to the air or vacuum surface. Therefore, the microphase separation generally occurs on the surfaces of the block copolymers and affects their bulk performances.[2–4] Furthermore, the morphological configuration of block polymers depends on the parameters mentioned above and many unique microphase strucures are possible, giving rise to a variety of properties.[2] Accordingly, many functional block copolymers have been synthesized.[3–10]

On the other hand, siloxane polymers and fluorinated polymers are two families of low surface energy materials. There were lots of investigations focusing on modifying the surfaces of the polymers using siloxane polymers that have low surface energy or/and fluorinated polymers to obtain the surface microphase separation structures.[8–13] However, previous studies in this field mainly focused on the fluorinated polymers or polymers with poly(dimethylsiloxane) (PDMS) segments.[8–14]

Recently, we synthesized a series of PDMS-*block*-poly(2,2,3,3,4,4,4-heptafluorobutyl methacrylate) (PDMS-*b*-PHFBMA) diblock copolymers using commercially available materials by atom transfer radical polymerization (ATRP) and the microphase separation behavior on their surfaces was also investigated.[15,16] The results proved that the diblock copolymers are well-defined polymers with microphase separation surfaces consisting of hydrophobic domain from PDMS segments and rather more hydrophobic domain from PHFBMA segments.[16] In addition, to get triblock copolymers with low surface energy and decrease the fluorine content in the

Correspondence to: Z.-H. Luo (luozh@xmu.edu.cn).
Contract grant sponsor: The "Eleventh Five-Year" scientific research Project of PLA; contract grant number: 08G026.

copolymers as much as possible due to the high price of the fluorineated polymers/monomers, we also synthesized a series of PDMS-*block*-poly(methyl methacrylate) (PMMA)-*block*-PHFBMA (PDMS-*b*-PMMA-*b*-PHFBMA) triblock copolymers via ATRP.[17] In our preliminary study,[17] we found that the surface energy of PDMS-*b*-PMMA-*b*-PHFBMA triblock copolymers can reach much lower than that of PDMS-*b*-PHFBMA diblock copolymers, despite of containing the same fluorine content in bulk. Corresponding X-ray photoelectron spectroscopy (XPS) characterization was also done to demonstrate the above difference. However, the surface morphological configurations of the triblock copolymers synthesized were not mentioned.[17]

In this work, we investigated the microphase separation behavior on the surfaces of the PDMS-*b*-PMMA-*b*-PHFBMA triblock copolymers with transmission electron microscopy (TEM), atomic force microscopy (AFM), and XPS, respectively. The effects of PHFBMA content on the surface microphase separation were studied. Comparison between the PDMS-*b*-PMMA-*b*-PHFBMA triblock copolymers and the PDMS-*b*-PHFBMA diblock copolymers was also done.

EXPERIMENTAL

The PDMS-*b*-PHFBMA and PDMS-*b*-PMMA-*b*-PHFBMA block copolymers were synthesized via ATRP according to our previous works.[15–17] Thereout, the resultant triblock copolymers were disposed and analyzed based on the following descriptions:[15–17]

Fourier transform infrared analysis

FTIR analysis was performed on an Avatar 360 FTIR spectrometer (Nicolet Instruments, Madison, WI). The spectrum was recorded before 32 times scanning at a resolution of 4 cm^{-1}.

^{1}H NMR analysis

The samples were dissolved in deuterated chloroform (free of TMS), and the nuclear magnetic resonance (NMR) spectra were measured on a Bruker AV400 NMR spectrometer.

Transmission electron microscopy observation

The morphology of the block copolymers was observed by TEM. The equilibrium film surface was obtained from the slow evaporation technique. A 25 mL cup of THF was placed in a dry seal desiccator to form a solvent atmosphere. A drop of 3 wt % polymer solution was applied onto a copper grid coated with carbon, and then the grid was placed in the dry seal desiccator for 72 h to eliminate trace solvent. The sample was used without any staining procedure. A transmission electron microscope (Tecnai F30) was used with an accelerating voltage of 300 kV.

Atomic force microscopy observation

AFM observation was made on 5500ILM Atomic Force Microscope (Agilent, USA) in noncontact mode under ambient conditions (25°C, 40% RH), using the microfabrication cantilevers with a spring constant of approximately 20 Nm^{-1}. All AFM data including the topographical and the three-dimensional (3D) image as well were recorded simultaneously. The films for the AFM measurements were prepared with a single drop of copolymer solution in THF on freshly cleaned Si wafer. Thickness of the films is about 20–50 μm. The samples for AFM measurements were dried in vacuum at room temperature.

Xps detection

XPS spectra were recorded with a PHI quantum 2000 scanning ESCA microprobe (physical electronic, USA), equipped with an Al $K\alpha_{1,2}$ monochromatic source of 1486.60 eV. The beam was 200 μm in diameter and the analysis area was 1.5 mm × 0.2 mm. The measurements were typically operated at 35 W. A typical multiplex pass energy was 29.35 eV, and a typical survey pass energy was 187.85 eV. The take off angle was 45°. Narrow scan spectrometer of C 1s, O 1s, F 1s, and Si 2p were collected and peak analysis was carried out using software. The basic vacuum was 5×10^{-8} Pa, whereas XPS spectra were taken up at 5×10^{-7} Pa. XPS samples were prepared using the following methods. The block copolymers were dissolved in THF, then were casted onto freshly cleaned aluminum foil and dried in a vacuum at room temperature.

Contact angle and surface energy measurements

The contact angle and surface energy were obtained by SL-200B measurement (Suolun, China) as reported contact angle was an average of five individual measurements on different regions of the same sample. The films for contact angle and surface free energy measurements were prepared by casting the copolymer solution onto clean glass slides. All samples were dried in vacuum at room temperature for 24 h. The surface energy of the films was calculated by Owens–Wendt method. The equilibrium contact angle is well defined by Young's equation:[3,18]

$$\sigma_s = \sigma_{sl} + \sigma_l \cos\theta, \quad (1)$$

where, σ_s, σ_1 and σ_{sl} are the interfacial free energies at solid–vapor, liquid–vapor, and solid–liquid interfaces, respectively. θ is the contact angle of liquid on a solid surface. Owens and Wendt proposed the division of the total surface energy in two components: the dispersive component (σ^d) and polar component (σ^p).[18] The dispersive component accounts for Van der Waals and other nonsite specific interactions and the polar component accounts for dipole–dipole, dipole–induced dipole, hydrogen bonding, and other site-specific interactions. Hence, interfacial free energies for σ_s and σ_l can be expressed as follows:[3,18]

$$\sigma_s = \sigma_s^d + \sigma_s^p, \tag{2}$$

$$\sigma_l = \sigma_l^d + \sigma_l^p, \tag{3}$$

where, σ_s^d and σ_s^p are the dispersive and polar contribution to the surface energy for the solid, σ_l^d and σ_l^p for the liquid, respectively. The interfacial energy (σ_{sl}) can be calculated from σ_s and σ_l based on the geometric mean method by the following equation:[3]

$$\sigma_{sl} = \sigma_s + \sigma_l - 2\left(\sqrt{\sigma_s^d\sigma_l^d} + \sqrt{\sigma_s^p\sigma_l^p}\right), \tag{4}$$

substituting of the σ_{sl} in eq. (1) with eq. (4), we get:

$$\sigma_l(1+\cos\theta) = 2\left(\sqrt{\sigma_s^d\sigma_l^d} + \sqrt{\sigma_s^p\sigma_l^p}\right), \tag{5}$$

substituting of the σ_l in eq. (5) with eq. (3), we get:

$$(\sigma_l^d + \sigma_l^p)(1+\cos\theta) = 2\left(\sqrt{\sigma_s^d\sigma_l^d} + \sqrt{\sigma_s^p\sigma_l^p}\right). \tag{6}$$

If the contact angles of two different liquids on the same polymer surface are known, and σ_s^d and σ_s^p can be obtained from eq. (6), and thus the surface free energy of the polymer film can be calculated by eq. (2). In this study, deionized water and ethylene glycol (EG) were selected as the probe liquid to determine the surface free energies of copolymer films. The values of σ_l^d (21.80 mN m^{-1}) and σ_l^p (51.00 mN m^{-1}) for water and σ_l^d (30.90 mN m^{-1}) and σ_l^p (16.80 m*N* m^{-1}) for EG were used in the calculation by SL-200B software. Substituting all known data above into eq. (6), the surface free energy of the copolymer film can be calculated by the following equation:

$$\sigma_s = \sigma_s^d + \sigma_s^p = \frac{\left(47.70\sqrt{51.00}(1+\cos\theta_{EG}) - 72.80\sqrt{16.80}(1+\cos\theta_{water})\right)^2}{4\left(\sqrt{1575.9} - \sqrt{366.24}\right)^2} + \frac{\left(72.80\sqrt{30.90}(1+\cos\theta_{water}) - 47.70\sqrt{21.80}(1+\cos\theta_{EG})\right)^2}{4\left(\sqrt{1575.9} - \sqrt{366.24}\right)^2}, \tag{7}$$

where, Θ_{EG} and Θ_{water} are the contact angles of EG and water on the same copolymer surface, respectively.

RESULTS AND DISCUSSION

Synthesis of PDMS-*b*-PMMA-*b*-PHFBMA triblock copolymers

A series of PDMS-*b*-PMMA-*b*-PHFBMA triblock copolymers were firstly synthesized by ATRP in order to observe the surface properties of the PDMS-*b*-PMMA-*b*-PHFBMA triblock copolymers, especially their microphase separation behavior. The synthetic scheme was shown in Scheme 1. Concerning the synthesis of PDMS-*b*-PMMA-*b*-PHFBMA triblock copolymers, readers are encouraged to refer to our past work.[17] Here we only provide typical ^{1}H-NMR and FTIR spectra to characterize the structure of PSMA-*b*-PMMA-*b*-PHFBMA triblock copolymer.

Typical ^{1}H-NMR spectrum and FTIR spectrum obtained in our group were shown in Figures 1 and 2, respectively. The dimethylsiloxane repeat unit of PDMS segments, the —OCH_3 group of PMMA block, and the —$OCH_2(CF_2)_2CF_3$ group of PHFBMA block give three characteristic peaks in NMR spectra as shown in Figure 1, centered at 0.00, 3.63, and 4.43 ppm, respectively. The other chemical shift assignments are also shown in Figure 1. Figure 2 shows the FTIR spectrum of the PDMS-*b*-PMMA-*b*-PHFBMA triblock copolymers and it also proves that the copolymer PDMS-*b*-PMMA-*b*-PHFBMA has been successfully synthesized. The adsorption at 1735 cm^{-1} is attributed to stretching vibrations of the C=O group of the PMMA block and the PHFBMA segments. The stretching vibrations of the C—O—C group appear at 1158 and 1264 cm^{-1}. The peaks appearing between 2880 cm^{-1} and 2968 cm^{-1} are assigned to stretching vibrations of the $-CH_3$ and $-CH_2$ groups. The characteristic peaks of the PDMS block appear between 1022 and 1112 cm^{-1}. As a whole, the measuring results prove that the PDMS-*b*-PMMA-*b*-PHFBMA triblock copolymers were successfully synthesized.

Microphase separation behavior

AFM experiments are routinely used to study the microphase-separated morphologies of block

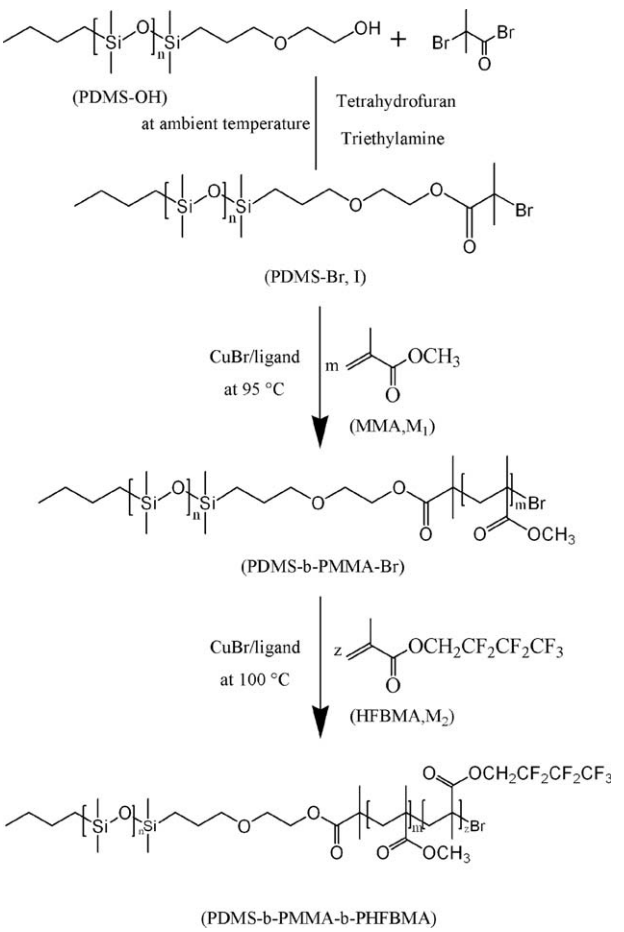

Scheme 1 Synthetic scheme for the preparation of PDMS-b-PMMA-b-PHFBMA triblock copolymers.

copolymers, where the size and shape of the microdomains are restricted to the block dimensions.[19–22] A noncontact AFM mode was used to image the surface topography of the copolymers.

Figure 3 shows the typical AFM images of the triblock copolymer $DMS_{65}MMA_{10}HFBMA_{30}$ films. The rough topography and three-dimensional (3D) image exhibited across surface are believed to be the result of the microphase separation. In addition, we can also obtain the following data via using the software along with 5500ILM Atomic Force Microscope: the highest height of the protuberant area in Figure 3**(b)** is 12.2 nm, the size of the discontinuous phase is about 400 nm, and root mean square (RMS) roughness in an area of $5 \times 5\ \mu m^2$ of this sample is 3.35 nm. Above AFM data must be explained along with TEM observation. Therefore, we also obtained the typical TEM images of the triblock copolymer films.

TEM observation is used to prove the surface microphase separation in the PDMS-*b*-PMMA-*b*-PHFBMA triblock copolymers. Figure 4 exhibits distinct phase-separated morphology of the triblock copolymer $DMS_{65}MMA_{10}HFBMA_{30}$ films composed of dark and bright domains. It is well-known that PDMS is hydrophobic and fluorine-containing polymer is even more hydrophobic than PDMS. Furthermore, we have shown that surface microphase separation in PDMS-*b*-PHFBMA block copolymers occurs.[16] As silicon in PDMS segments has a higher electron density than the carbon atoms in PMMA and PHFBMA, the dark regions of the TEM bright-field micrograph in Figure 4 represent the PDMS domains. Thus, it can be concluded that PMMA and more hydrophobic PHFBMA patches appear bright in TEM. In practice, one knows that the size of microphase-separated structure is controllable by change in the each block length. The structure itself as well as the size of microphase-separated domains can also be controlled by the ratio of two block sequences, incorporation of another component (triblock copolymer), and so on. Also, the triblock structure will restrict the segregation of lower surface free energy components at the film surface, resulting in the formation of the lateral phase separation.[23] So the introduction of the PMMA segments may promote the fluorine segregation onto the surface. Furthermore, the bright area was primarily composed of the PMMA segments and the PHFBMA segments.

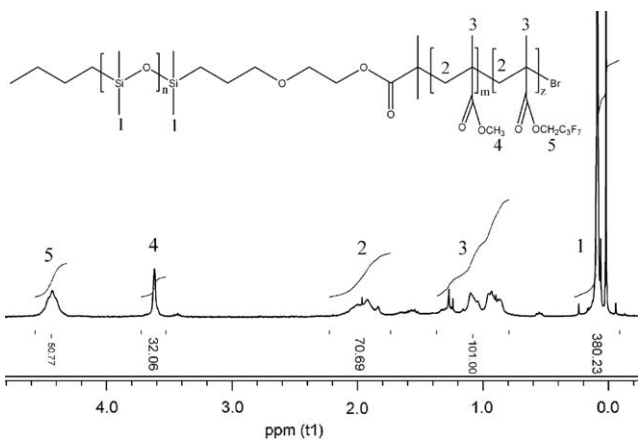

Figure 1 ^{1}H-NMR spectrum of PDMS-PMMA-PHFBMA triblock copolymers (No.1).

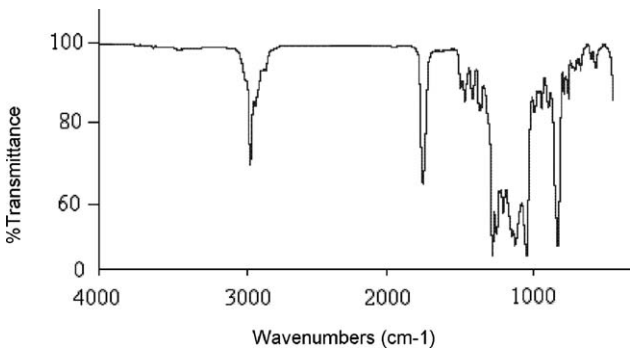

Figure 2 FTIR spectra of PDMS-PMMA-PHFBMA triblock copolymers (No.1).

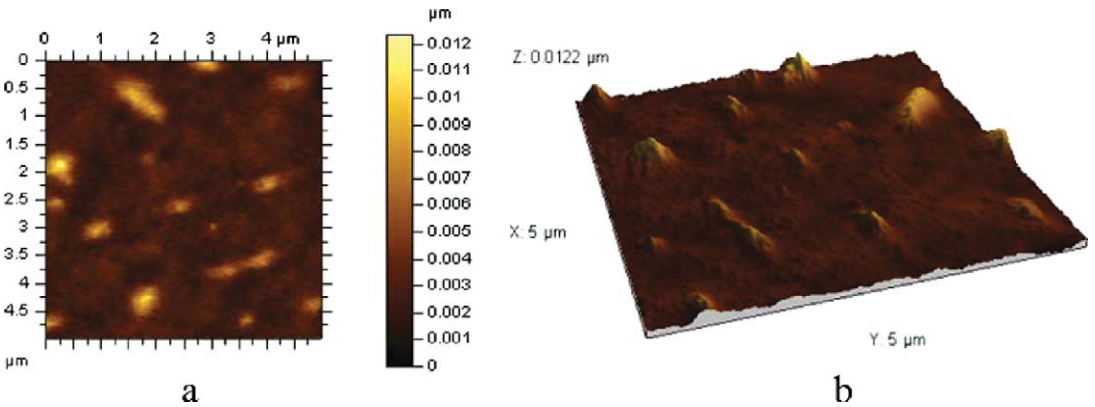

Figure 3 The AFM topography image and 3D image of DMS65MMA10HFBMA30 copolymer films (No.1) (a. AFM topography image; b. 3D image). [Color figure can be viewed in the online issue, which is available at wileyonlinelibrary.com.]

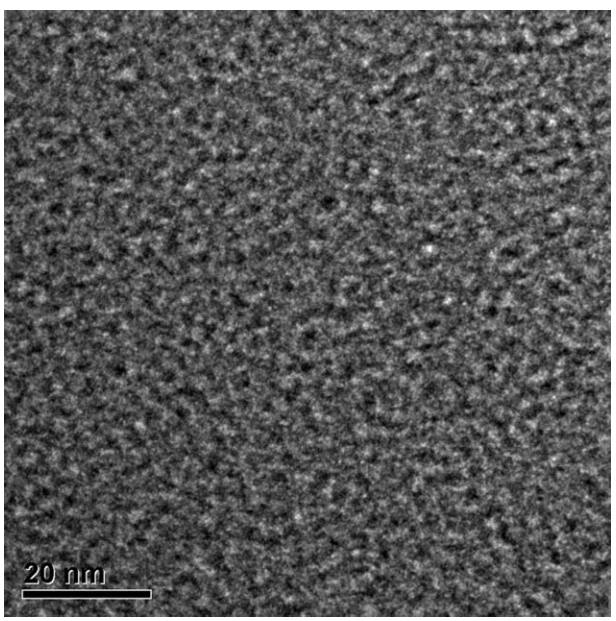

Figure 4 The TEM micrograph of DMS65MMA10HFBMA30 copolymer films (No.1).

Effects of PHFBMA content

Figures 3, 5–7 describe the AFM topography images of the triblock copolymer films with different compositions. They show that with the increase of the PHFBMA content, more PHFBMA segments seem to immigrate to the surface, and more distinct phase interfaces are observed. Simultaneously, the roughness data computed by software along with 5500ILM Atomic Force Microscope (Table I) show that the roughness of the samples increases with the increase of the PHFBMA content, suggesting that further segment segregation happens with the increase of the PHFBMA content.

The evolution of the surface morphology with the increase of the polymerization degree of PHFBMA can be caused by the enrichment of PHFBMA segments at the copolymer-air interface and the reorganization of PDMS phase, which can also be further confirmed by XPS detection. The XPS images of the four samples obtained are very alike with each other and represent different surface atomic ratios of F/Si computed by software. The obtained surface atomic ratio of F/Si is also shown in Table I. Here we only

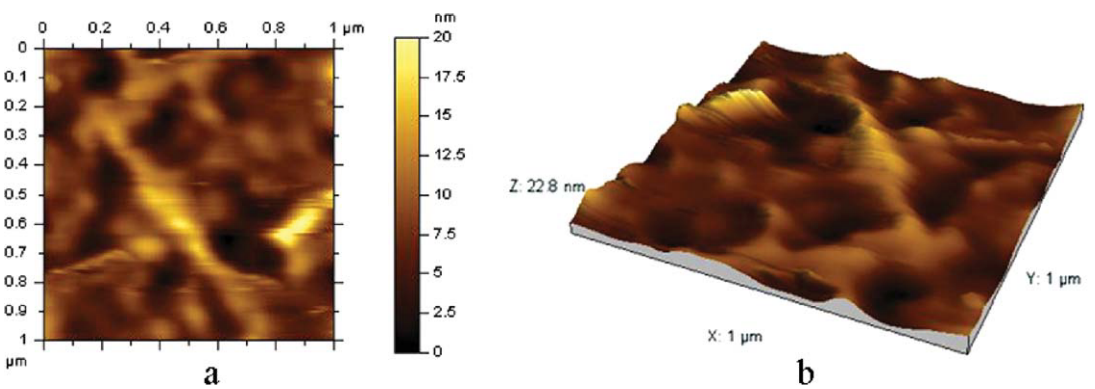

Figure 5 The AFM topography image and 3D image of DMS65MMA10HFBMA20 copolymer films (No.2) (a. AFM topography image; b. 3D image). [Color figure can be viewed in the online issue, which is available at wileyonlinelibrary.com.]

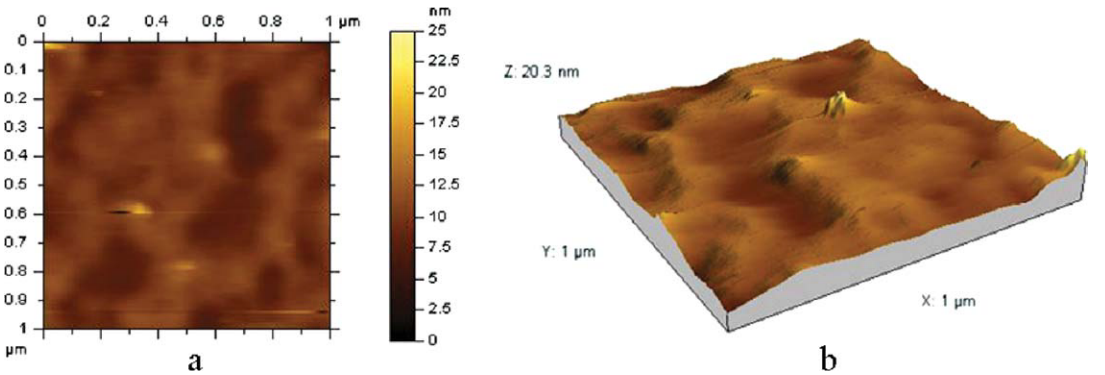

Figure 6 The AFM topography image and 3D image of DMS65MMA10HFBMA10 copolymer films (No.3) (a. AFM topography image; b. 3D image). [Color figure can be viewed in the online issue, which is available at wileyonlinelibrary.com.]

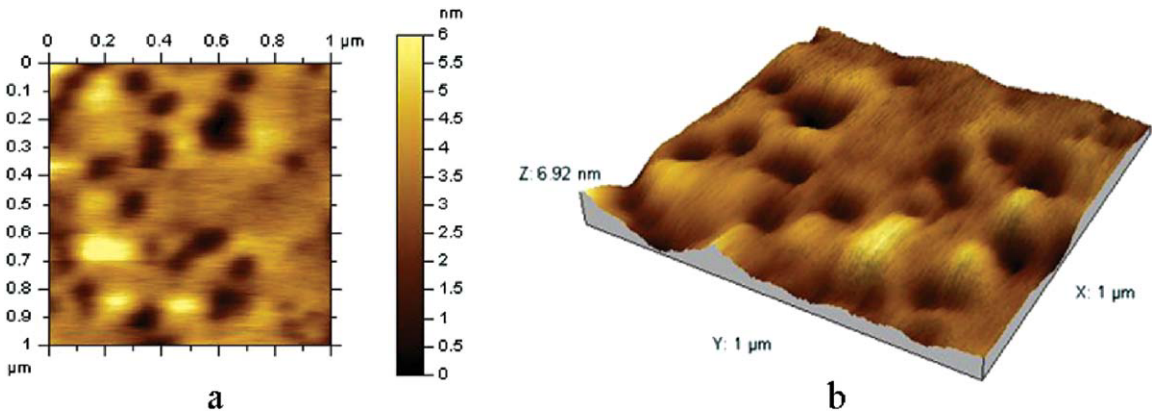

Figure 7 The AFM topography image and 3D image of DMS65MMA3HFBMA6 copolymer films (No.4) (a. AFM topography image; b. 3D image). [Color figure can be viewed in the online issue, which is available at wileyonlinelibrary.com.]

TABLE I
The Surface Compositions and Roughness of PDMS-*b*-PMMA-*b*-PHFBMA triblock Copolymers dependent on the PHFBMA Content 27

Sample Nos.	$DMS_xMMA_yHFBMA_z$	W_{PHFBMA}[a] (%)	$M_{n,theo}$[b] (g/mol)	$M_{n,NMR}$[c] (g/mol)	$M_{n,GPC}$[d] (g/mol)	PDI[e]	F/Si[f]	Roughness[g] (nm)
1	$DMS_{65}MMA_{10}HFBMA_{30}$	58.3	14,760	14,600	15,100	1.23	5.23	3.35
2	$DMS_{65}MMA_{10}HFBMA_{20}$	48.3	11,890	11,750	12,200	1.13	3.90	1.97
3	$DMS_{65}MMA_{10}HFBMA_{10}$	31.8	9020	8900	9200	1.15	2.68	1.15
4	$DMS_{65}MMA_3HFBMA_6$	24.0	7172	7100	7500	1.09	1.06	0.974
5	$DMS_{65}HFBMA_{25}$	58.2	12,325	12,300	12,600	1.18	0.92	2.00

[a] W_{PHFBMA} represents the weight percent of the PHFBMA block calculated by the equation: PHFBMA % = $(287 \times DP_{n(HFBMA)})/(5150 + 100 \times DP_{n(MMA)} + 287 \times DP_{n(HFBMA)})$.
[b] $M_{n,theo}$ represents the theoretical molecular weight.
[c] The molecular weight was measured by ^{1}H-NMR (three distinctive peaks in the ^{1}H-NMR spectrum (Fig. 1) can be assigned to hydrogen of the —OCH_2— group at 4.43 ppm affected by the ester group in HFBMA, hydrogen of the —OCH_3 group at 3.62 ppm affected by the ester group in MMA, and the dimethylsiloxane repeat units at 0.0–0.2 ppm, respectively. Integral ratio of the three regions can be used to calculate number-average molecular weight (M_n) values: $M_n = 5150 + 100 \times DP_{n(MMA)} + 287 \times DP_{n(HFBMA)}$).
[d] The molecular weight was measured by GPC.
[e] The polydispersity of the copolymers were measured by GPC, which was performed using THF as the eluent at a flow rate of 1 mL min^{-1} with a series of polystyrene standards as the reference.
[f] The surface atomic ratio of F/Si of the copolymer films was determined by XPS.
[g] The roughness of the copolymer films was obtained via the AFM software.

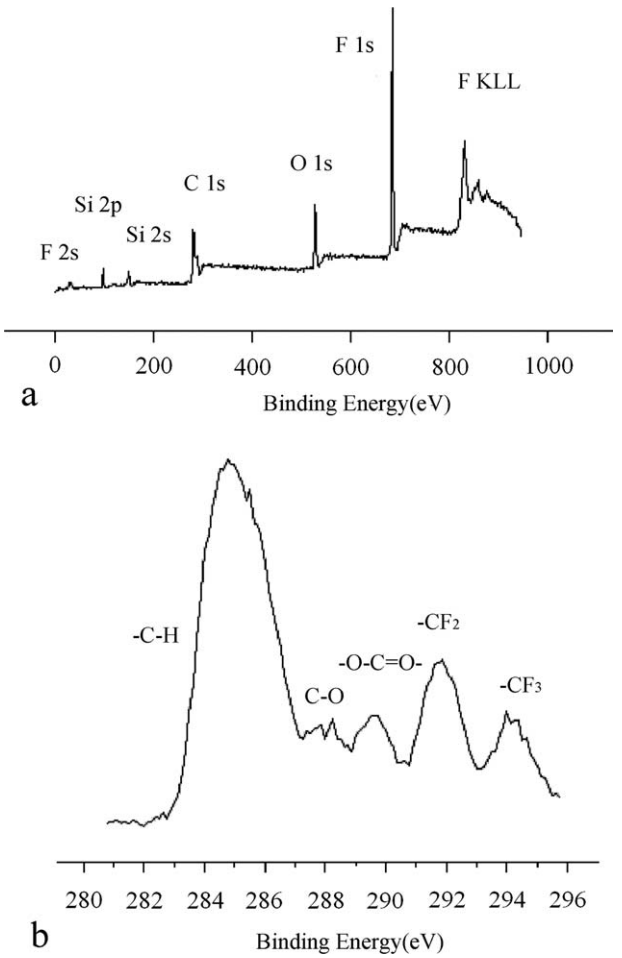

Figure 8 XPS of DMS65MMA10HFBMA30 copolymer films (No.1) (a. broad scan of the BE spectrum; b. high-resolution C 1s spectrum).

supply the typical XPS images of **Sample No.1**. The XPS images with peak assignment for the surface compositions of the PDMS-*b*-PMMA-*b*-PHFBMA triblock copolymer sample were shown in Figure 8. From Table I, it can be seen that with the decrease of atomic ratio of F/Si, less and less fluorine were detected on the surface of these copolymer samples while the AFM imaging of them were getting smoother and smoother.

Surface energies of triblock copolymer films

The total surface energies (σ_s) along with the polar and dispersive contributions to the surface energy of the triblock copolymers with different polymerization degrees are determined and given in Table II. Compared with the surface energies of the block copolymer films, it is obvious that all the block copolymer films provide a surface energy of as low as 5–40 mN/m. And the contact angle increases with the increase of polymerization degree of PHFBMA.

TABLE II
The Static Water Contact Angles of the PDMS-*b*-PMMA-*b*-PHFBMA triblock Copolymers Dependent on the PHFBMA Content

Sample Nos.	$DMS_xMMA_yHFBMA_z$	$\theta_{(H_2O)}$ (°)	σ_s[a] (mN/m)
1	$DMS_{65}MMA_{10}HFBMA_{30}$	136.20	4.51
2	$DMS_{65}MMA_{10}HFBMA_{20}$	120.31	11.43
3	$DMS_{65}MMA_{10}HFBMA_{10}$	111.87	16.01
4	$DMS_{65}MMA_3HFBMA_6$	75.32	38.41
5	$DMS_{65}HFBMA_{25}$	121	11.10

[a] The values are obtained from a telescopic goniomete (SL-200B), and σ_s represents the surface energy of the PDMS-*b*-PMMA-*b*-PHFBMA triblock copolymers.

Here, in order to study the effect of PMMA segments, we compared the surface behavior in the PDMS-*b*-PMMA-*b*-PHFBMA triblock copolymers with that in the PDMS-*b*-PHFBMA diblock copolymers. The PDMS-*b*-PHFBMA diblock copolymers were also synthesized by ATRP. Concerning the synthesis and structure characterization of PDMS-*b*-PHFBMA diblock copolymers, readers are encouraged to refer to our past work.[15,16] Furthermore, here, we point out that the selected samples, namely **No.1** and **No.5** shown in Tables I and II, contain approximately equal fluorine content in their bulks. Corresponding results were also listed in Tables I and II. Tables I and II show that the addition of PMMA segments can increase the static water contact angle from 121 to 136°, which not only depends on their surface compositions but also on their surface morphologies. XPS spectra were used to measure their surface compositions and results were listed in Table III. In addition, AFM data were obtained and shown in Figures 3 and 9, respectively.

Table III shows that for the diblock copolymer samples and the triblock copolymer samples, the surface F/Si atomic ratio increases from 0.92 to 5.32, corresponding to the increase of static water contact angle from 121 to 136°. XPS characterization (not present here) indicates that the molecular structure has an effect on the fluorine segregation.[17] In

TABLE III
Surface Compositions of Fluorosilicone Block Copolymers Measured by XPS

Sample Nos	$DMS_xMMA_yHFBMA_z$	*F* (%) in bulk	C 1s(%)	O 1s (%)	Si 2p (%)	F 1s (%)	F/Si
1	$DMS_{65}MMA_{10}HFBMA_{30}$	28.1	36.0	19.9	7.1	37.0	5.23
5	$DMS_{65}HFBMA_{25}$	28.0	23.0	24.0	25.5	23.5	0.92

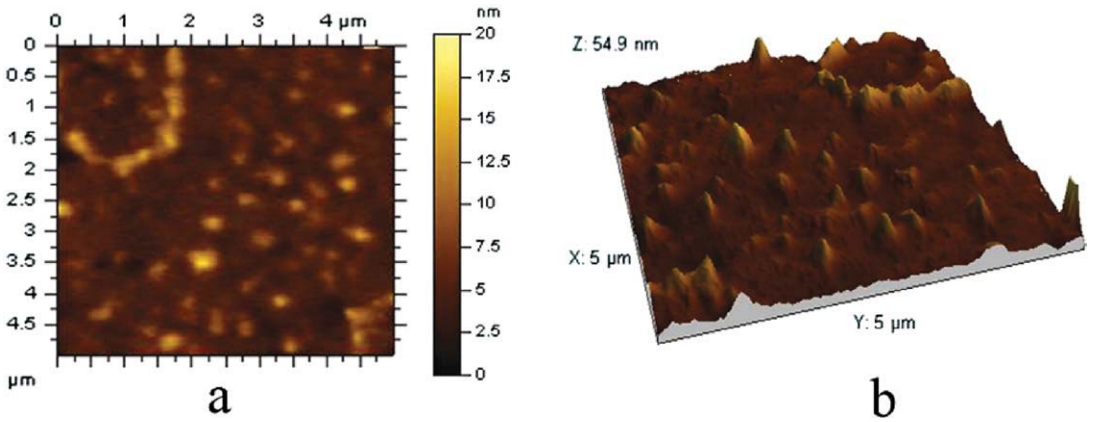

Figure 9 The AFM topography image and 3D image of DMS65HFBMA25 copolymer films (No.5) (a. AFM topography image; b. 3D image). [Color figure can be viewed in the online issue, which is available at wileyonlinelibrary.com.]

addition, Figures 3 and 9 obviously prove that the surface microphase separation exists in the PDMS-*b*-PMMA-*b*-PHFBMA triblock copolymer films and the PDMS-*b*-PHFBMA diblock copolymer films. Furthermore, the obtained RMS roughness of the triblock copolymer sample is greater than that of the diblock copolymer sample. Corresponding data were listed in Table I. For the PDMS-*b*-PHFBMA diblock copolymer sample, comparing to the hydrophobic PDMS segments, the more hydrophobic PHFBMA segments preferentially segregate to the air-side surface or vacuum surface.[16] Combining the above XPS and AFM data, one can know that the fluorine enrichment at the air-side surface of two copolymers increases with more obvious microphase separation. In our opinion, microphase separation makes the low surface energy parts in the bulk more easily tend to segregate to the surface, results in more fluorine enrichment, and gives stronger hydrophobicity.[17,24] So the introduction of the PMMA block promotes the fluorine segregation onto the surface and decrease the fluorine content in the copolymers with low surface energy.

CONCLUSIONS

The microstructure of the block copolymers was investigated by transmission electron microscopy (TEM) and atomic force microscopy (AFM). Surface composition was studied by X-ray photoelectron spectroscopy (XPS). The results prove that the triblock copolymers are well-defined polymers with microphase separation surfaces consisting of hydrophobic domain from PMMA segments and rather more hydrophobic domain from PDMS segments and PHFBMA segments. Furthermore, the effects of the PHFBMA content on the microphase separation behavior were investigated. The results show that the increases of the PHFBMA content can strengthen the microphase separation in PDMS-*b*-PMMA-*b*-PHFBMA triblock copolymers. Comparison between the PDMS-*b*-PMMA-*b*-PHFBMA triblock copolymers and the PDMS-*b*-PHFBMA diblock copolymers shows that the introduction of the PMMA block promotes the fluorine segregation onto the surface and decreases the fluorine content in the copolymers with low surface energy both because of their surface compositions and their surface morphologies.

The authors acknowledge the State Key Laboratory of Physical Chemistry of Solid Surfaces at Xiamen University for providing AFM facilities and assistance.

References

1. Reiss, G. In Encyclopedia of Polymer Science and Engineering, Kroschwitz, J. I., Ed.; Wiley-Interscience: New York, 1988; pp 324–328.
2. Patel, N. M.; Dwight, D. W.; Hedrich, J. L.; Webster, D. C.; McGrath, J. E. Macromolecules 1988, 21, 2689.
3. Fang, H. X.; Zhou, S. X.; Wu, L. M. Appl Surf Sci 2006, 253, 2978.
4. Olemskoi, A.; Savelyev, A. Phys Rep 2005, 419, 145.
5. Verploegen, R.; Boone, D.; Hammond, P. T. J Polym Sci Part B: Polym Phys 2007, 45, 3263.
6. Huang, L.; Yuan, H.; Zhang, D. B.; Zhang, Z.; Guo, J.; Ma, J. M. Appl Surf Sci 2004, 225, 39.
7. Bes, L.; Huan, K.; Khoshdel, E.; Lowe, M. J.; McConville, C. F.; Haddleton, D. M. Eur Polym J 2003, 39, 5.
8. Fang, H. X.; Feng, L. B.; You, B.; Wu, L. M. J Polym Sci Part B: Polym Phys 2007, 45, 208.
9. Ku, C. K.; Lee, Y. D. Polymer 2007, 48, 3565.
10. Saïdi, S.; Guittard, F.; Guimon, C.; Géribaldi, S. Eur Polym J 2006, 42, 702.
11. Luo, Z. H.; Yu, H. J.; He, T. Y. J Appl Polym Sci 2008, 108, 1201.
12. Gudipati, C. S.; Greenlief, C. M.; Johnson, J. A.; Prayongpan, P.; Wooley, K. L. J Polym Sci Part A: Polym Chem 2004, 42, 6193.
13. Person, D. V.; Fitch, J. W.; Cassidy, P. E.; Kono, K.; Reddy, V. S. React Funct Polym 1996, 30, 141.

14. Majumdar, P.; Webster, D. C. Macromolecules 2005, 38, 5857.
15. Luo, Z. H.He, T. Y. React Funct Polym 2008, 68, 931.
16. Luo, Z. H.; Yu, H. J.; Zhang, W. J Appl Polym Sci 2009, 113, 4032.
17. Luo, Z. H.; He, T. Y.; Yu, H. J.; Dai, L. Z. Macromol React Eng 2008, 2, 398.
18. Owens, D. K.Wendt, R. C. J Appl Polym Sci 1969, 13, 1741.
19. Boltau, M.; Walheim, S.; Mlynek, J.; Krausch, G.; Steiner, U. Nature 1998, 391, 877.
20. Kajiyama, T.; Tanka, S. R.; Ge, S. R.; Takahara, A. T. Prog Surf Sci 1996, 52, 1.
21. Matsen, M. W.; Bates, F. S. J Chem Phys 1997, 106, 2436.
22. Spatz, J. P.; Eibeck, P.; Mobmer, S.; Moller, M.; Herzog, T.; Ziemann, P. Adv Mater 1998, 10, 849.
23. Kojio, K.; Uchiba, Y.; Mitsui, Y.; Furukawa, M.; Sasaki, S.; Matsunaga, H.; Okuda, H. Macromolecules 2007, 40, 2625.
24. Hosoya, A.; Kurakami, G.; Narita, T.; Hamana, H. React Funct Polym 2007, 67, 1187.